J Therm Anal Calorim (2010) 99:123–138
DOI 10.1007/s10973-009-0500-y

Resolution of problems in soft matter dynamics by combining calorimetry and other spectroscopies

K. L. Ngai · S. Capaccioli · M. Shahin Thayyil · N. Shinyashiki

Japan Symposium 2008

Abstract In several current important problems in different areas of soft matter physics, controversy persists in interpreting the molecular dynamics observed by various spectroscopies including dielectric relaxation, light scattering, nuclear magnetic resonance, and neutron scattering. Outstanding examples include: (1) relaxation of water in aqueous mixtures, in molecular sieves and silica-gel nanopores, and in hydration shell of proteins; and (2) dynamics of each component in binary miscible polymer blends, in mixtures of an amorphous polymer with a small molecular glassformer, and in binary mixtures of two small molecular glassformers. We show the applications of calorimetry to these problems have enhanced our understanding of the dynamics and eliminated the controversies.

Keywords Glass transition · Thermal analysis · Adiabatic calorimetry · Water · Aqueous mixtures · Water in nano-confinement · Hydration water · Hydrated protein · Polymer blends · Polymer solutions

K. L. Ngai
Naval Research Laboratory, Washington, DC 20375-5320, USA

S. Capaccioli (✉) · M. Shahin Thayyil
Dipartimento di Fisica, Università di Pisa, Largo Bruno Pontecorvo 3, 56127 Pisa, Italy
e-mail: capacci@df.unipi.it

S. Capaccioli · M. Shahin Thayyil
CNR-INFM, PolyLab, Largo Bruno Pontecorvo 3, 56127 Pisa, Italy

M. Shahin Thayyil
Department of Physics, University of Calicut, Calicut, Kerala, India

N. Shinyashiki
Department of Physics, Tokai University, Hiratsuka, Kanagawa 259-1292, Japan

Introduction

Thermal analysis and calorimetry have proven to be important and useful research tools in many different fields. In the research on relaxation dynamics and glass transition in particular, calorimetry is perhaps the quintessential experimental method not only because the enthalpy relaxation characteristic of glass transition is observed, but also its time scale ranging from 10^6 to 10^2 s corresponds to the vitrification in the laboratory. Also, at this long timescales, different relaxation processes are more widely separated in temperature and clearly resolved. This distinct advantage over other spectroscopies probing dynamics at shorter time scales can make calorimetry useful to arrive at unequivocal interpretation of the dynamics of some soft matters, which cannot be achieved by the other spectroscopies acting alone. In this article, we consider several such systems, where despite extensive studies through various spectroscopies, including dielectric relaxation, light scattering, nuclear magnetic resonance, and neutron scattering, the interpretation of the dynamics is controversial. The soft matter systems considered are (1) water in aqueous mixtures, in molecular sieves and silica-gel nanopores, and in hydration layer of proteins; and (2) two miscible component systems including polymer blends, mixtures of an amorphous polymer with a small molecular glassformer, and in mixtures of two small molecular glassformers. First, we summarize the essential results from the other spectroscopies and the controversy of interpretation in each system, and then show how measurements by calorimetry and particularly adiabatic calorimetry have clarified the

dynamics, resolved the controversy, and made real progress in understanding the dynamics of the systems.

Dynamics of aqueous mixtures

Water is the most abundant and important soft matter. It has the simplest molecular structure, but ironically the interpretation of its relaxation dynamics has been most controversial in the past many decades of scientific research. Here, we discuss only some of the more recent experimental data of water in various situations obtained by different spectroscopies, and the different interpretations that are controversial. We start with the dielectric relaxation data of aqueous mixtures. All the collected data of many aqueous mixtures with various wt% of water show the presence of the α-relaxation of the solute hydrogen bonded with the water, and a secondary relaxation originating from the water component. (For a collection of data see [1].) The relaxation time of the α-relaxation, τ_α, has the Vogel-Fulcher-Tammann-Hesse (VFTH) T-dependence, typical of cooperative structural relaxation. For some aqueous mixtures, differential scanning calorimetry (DSC) measurements have been made and the calorimetric glass transition temperature, T_g, identified by a jump in heat capacity is about the same as the dielectric T_g defined as the temperature at which τ_α falls in the neighborhood of 10^2 or 10^3 s. As regards to the secondary relaxation originating from water in aqueous mixtures, the T-dependence of its relaxation time, τ_β, is Arrhenius below T_g and has activation enthalpy in the range of 40–50 kJ/mol [1], but it changes to a stronger dependence above T_g. Its dielectric strength, $\Delta\varepsilon_\beta$, also exhibits a change to a stronger increase with increasing T after crossing T_g. The fact that $\Delta\varepsilon_\beta$ increases with increasing T above T_g is clear evidence that the water-specific relaxation continues above T_g to be truly a secondary relaxation. This invalidates the suggestion by others that the observed water-specific relaxation at temperatures above T_g is either a merged α- and β-processes or simply the α-relaxation of water. The observed changes of the T-dependence of τ_β and $\Delta\varepsilon_\beta$ of water in aqueous mixtures are exactly analogous to that found in the secondary relaxation of a fast component in binary van der Waals liquids [1–5]. Moreover, both the α- and β-process of the fast component are present above T_g. The data of the latter systems particularly those obtained at elevated pressure have become so transparent that a satisfactory explanation has been given from the Coupling Model (CM). The secondary relaxation is identified as the primitive relaxation of the CM due to the good agreement between the observed τ_β and the primitive relaxation time τ_0. It also can be called the Johari-Goldstein (JG) β-relaxation of water since the latter is also a local process, supposedly also a universal feature of all glass-formers and its relaxation time, τ_{JG}, is nearly the same as τ_0 [2–7]. Naturally, from the exact analogy with binary van der Waals liquids, the observed faster process in aqueous mixtures is the primitive relaxation or the JG β-relaxation of water in the mixtures above and below T_g. There is, however, a subtle difference between aqueous mixtures and binary van der Waals liquids. While each component of binary van der Waal liquids has its own α- and JG β-relaxations distinctly different from each other, hydrogen bonding of water with the hydrophilic solute in aqueous mixtures forces the motions of the two components to be coupled together. Thus, both components are somehow involved in all the observed primary and secondary relaxations of aqueous mixtures. In particular, although we used before [1] and in this article the nomenclature, the primitive or JG β-relaxation of water, necessarily this motion of water is coupled to some local motion of the solute. Evidence of this coupling can be seen from the sensitive dependence of τ_{JG} and its activation energy of water on wt% of water in mixtures with glycerol [1], or water in mixtures with different solutes [1].

In the following sections, we shall see that primitive relaxation or the JG β-relaxation and the two equivalent relaxation times $\tau_{JG}(T) \approx \tau_0$, come up again and again because it is a fundamental process and hence ubiquitous. Data from precision adiabatic calorimetry confirm the same and, in the process, help to resolve controversy in theoretical interpretation of the dynamics of water and water-related systems.

The dynamics of water nano-confined in molecular sieves

The dynamics of water nano-confined in molecular sieves (MS) had been studied by means of dielectric spectroscopy [8]. In a cylindrical pore with diameter of 10 Å, two major relaxation processes were observed (see Fig. 2b in [8], and Fig. 1 of this article). According to the authors in Ref. [8], the much more intense slower process (open squares) is contributed by most of the water molecules in 10 Å pores, and is likely due to strong interactions with the hydrophilic inner surfaces of molecular sieves. Its relaxation time, τ_{sMS}, increases with decreasing temperature to attain 100 s at about 170 K. The relaxation time of the weak faster process, τ_{fMS} (closed blue squares), has Arrhenius temperature dependence at low temperatures below about 175 K. The magnitude of τ_{fMS} is nearly the same as the relaxation time $\tau_{6Å}$ (closed circles) of the 6 Å ultrathin water layer (two molecular layers) confined in fully hydrated Na-vermiculite clay measured by dielectric spectroscopy [9]. The Arrhenius temperature dependence of τ_{fMS} does not persist at higher temperatures, but change

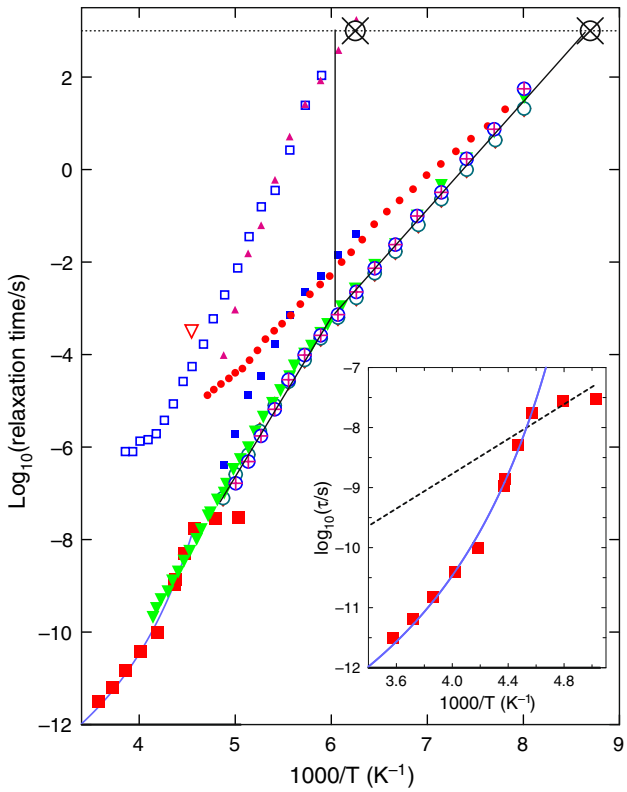

Fig. 1 Color online. τ_{sMS} and τ_{fMS}, of a slower (blue, *open square*) and faster (blue, *filled square*) relaxation of water confined in 10 Å molecular sieves [8]. τ_{fMS} changes to stronger temperature dependence above $T_g \approx 180$ K where $\tau_{sMS} \approx 10^3$ s. Dielectric data [11] of τ_{fMS} of water confined in MCM-41 with pore diameter 2.14 nm at hydration levels 12 wt% (*open circles*), 22 wt% (*inverted filled triangle*), 55 wt% (*open circles* with + inside). Change of *T*-dependence of τ_{fMS} made clear by two lines with different slopes. The *lone red inverted open triangle*: τ_{sMS} deduced from the dielectric spectrum at 220 K after subtracting off the conductivity. Relaxation time (*filled circle*) of 6 Å water in Na-vermiculite clay [9]. The two ⊗ are τ_{sMS} and $\tau_{fMS} = 10^3$ s of water confined within 1.2, 1.6 and 1.8 nm nano-pores of MCM-41 obtained by adiabatic calorimetry at $T = 115$ and 165 K respectively [18]. The *triangles* are τ_{sMS} calculated from τ_{fMS} by the CM. The *red closed squares* are translational relaxation time $\langle\tau_T\rangle$ determined by neutron scattering of water confined in nanoporous MCM-41-S with pore diameters of 14 Å. The same data are shown separately in the *inset*

to stronger temperature dependence at temperatures above 180 K. This crossover of temperature dependence of τ_{fMS} is the same as what we have seen in τ_{JG} of the JG-process in various non-aqueous and aqueous mixtures [1–5], and is a general property of JG β-relaxation. The striking similarity between this feature of τ_{fMS} and that shown by τ_{JG} leads us to interpret the observed faster process in a molecular sieve as the primitive relaxation or the JG β-relaxation of water and the associated slower process as the α-process of water strongly interacting with the hydrophilic inner surfaces of the molecular sieve. Such a relation between the two processes is further supported by applying the CM relation between τ_{JG} and τ_α [2–7] to the present case of τ_{fMS} and τ_{sMS} for water confined in 10 Å pores. Through the use of CM relation adapted for the present case,

$$\tau_{sMS}(T) = [t_c^{-n}\tau_{fMS}(T)]^{1/(1-n)}, \quad (1)$$

we calculate τ_{sMS} from the data of τ_{fMS} (closed triangles) by assuming $t_c \approx 2$ ps as other molecular glass-formers and $(1 - n) \equiv \beta_K = 0.69$. With this choice of the Kohlrausch exponent, $\beta_K = 0.69$, the calculated τ_{sMS} (closed triangles) are in approximate agreement with the experimental values (open squares) as shown in Fig. 1. The value of $\beta_K = 0.69$ chosen is not far from the value of 0.65 reported by Swenson et al. [10] as the Kohlrausch exponent obtained by means of quasi-elastic neutron scattering after averaging the result from various scattering vectors.

More recent dielectric data [11] of τ_{fMS} of water confined in molecular sieves MCM-41 C10 with pore diameter 2.14 nm at hydration levels with $H = 12$, 22, and 55 wt% are also shown in Fig. 1. The change of *T*-dependence of τ_{fMS} at temperature ≈ 166 K (location indicated by the vertical solid line) is made clear by the two lines to show that the data have different slopes above and below 166 K. The single open inverted triangle is the value of τ_{sMS} deduced from the dielectric spectrum at 220 K after subtracting off the conductivity.

The dynamics of water confined in nanoporous silica matrices MCM-41-S with pore diameters of 18 and 14 Å, have been studied down to 200 K by quasielastic neutron scattering. The data were analysed using a relaxing cage model by Faraone et al. [12, 13]. These authors determined the temperature variation of the average translational relaxation time $\langle\tau_T\rangle$ and found it exhibiting an abrupt change from VFTH-like at higher temperatures to Arrhenius law at $T \approx 225$ K with activation energies of 5.28 and 6.72 kcal/mol for 18 and 1.4 Å size pores, respectively. They interpreted this behavior as the fragile-to-strong liquid–liquid transition of water, involving $\langle\tau_T\rangle$ of the structural α-relaxation of nano-confined water. Their data (red closed squares) are plotted in Fig. 1 and shown separately in the inset of Fig. 1. Similar behavior was observed in the *T*-dependence of the reciprocal of the self-diffusion coefficient of water confined in cylindrical nanoporous matrices (MCM-41-S) with 14 Å pores [14].

As can be seen in Fig. 1, the neutron $\langle\tau_T\rangle$ with the VFTH dependence seems to be continuation of the dielectric τ_{fMS} of water confined in molecular sieves MCM-41 C10 with pore diameter 2.14 nm at hydration levels with $H = 12$ wt% (open circles), 22 wt% (closed inverted green triangles), 55 wt% (open circles with + inside). However, inference from dielectric measurement indicate that τ_{fMS} is the secondary relaxation of water, and

hence also that of the neutron $\langle\tau_T\rangle$. Thus, the neutron scattering experiments did not observe the α-relaxation of supercooled water above 225 K, but instead the primitive or JG β-relaxation of water. Moreover, if the Arrhenius T-dependence of the neutron $\langle\tau_T\rangle$ of [12] and [13] at ambient pressure were extrapolated to temperatures below 225 K this would indicate that glass transition of nano-confined water occurs at around 50 K when $\langle\tau_T\rangle = 10^2$ s according to Swenson [15], and 80 K when $\langle\tau_T\rangle = 10^3$ s according to Oguni et al. [16]. Such low glass-transition temperatures are in conflict with all literature data on glass-transition of supercooled water [17]. This again indicates that the measured neutron $\langle\tau_T\rangle$ for $T < 225$ K is unrelated to the α-relaxation of the supercooled confined water.

On the contrary, τ_{fMS} exhibits no abrupt change to Arrhenius dependence anywhere near 225 K, although there is one found near 166 K as we mentioned before. There is support from most recent adiabatic calorimetry data of our interpretation that τ_{fMS} is the primitive or JG β-relaxation time of water, and it changes its T-dependence at near 166 K where τ_{sMS} of the α-relaxation is 10^3 s. Adiabatic calorimetry measurements of the enthalpy relaxation of water confined within MCM-41 nano-pores were made by Oguni et al. [18].[1] Again, a slower and a faster relaxation of water confined within 1.2-nm nano-pores of silica MCM-41 have been found. Their relaxation times, τ_{sMS} and τ_{fMS}, have the value of 10^3 s at $T = 115$ and 165 K, respectively, and are shown in Fig. 1 by the two larger circles (⊗). The temperature location of $\tau_{sMS} = 10^3$ s from adiabatic calorimetry in Fig. 1 is 165 K. This is about the same as that of τ_{sMS} (blue open squares) at 10^3 s from dielectric relaxation of water confined in molecular sieves with pore diameter of 10 Å [8]. The temperature location of $\tau_{fMS} = 10^3$ s from adiabatic calorimetry is 115 K. This temperature also is nearly the same as that obtained by extrapolating the Arrhenius dependence of τ_{fMS} determined by dielectric relaxation [11] to 10^3 s, as demonstrated in Fig. 1. The agreement shows that τ_{fMS} from both methods belong to the same process. Interestingly, this process of water in molecular sieves has about same activation enthalpy as τ_{JG} of the 50% water mixtures with PVME, PVP, and other aqueous mixtures shown in [1], as well as $\tau_{6Å}$ of the 6 Å water layer confined in fully hydrated Na-vermiculite clay. Moreover, the τ_{fMS} from adiabatic calorimetry located at $T = 115$ K is nearly the same as the value obtained by extrapolation of the Arrhenius dependence of τ_{JG} of the 50% water mixtures with PVME or with PVP to lower temperatures [1]. These coincidences indicate that τ_{fMS} from dielectric relaxation and adiabatic calorimetry is an intrinsic feature of water, i.e., its primitive relaxation or JG β-relaxation, present in mixtures and in nano-confinement.

The dynamics of water nano-confined in silica gels and hydrogels

Since the primitive relaxation or JG β-relaxation of water is an intrinsic process, its characteristics should not be sensitive to other modes of nano-confinement including silica hydrogels [19], hydrogel of PHEMA [20–23], and in pores of silica gels [16]. Two relaxation processes of pure water confined in aged silica hydrogels were also observed dielectrically [19]. Their relaxation times are shown in Fig. 2 as a function of reciprocal temperature. The relaxation time, τ_{fC}, of the faster relaxation has Arrhenius temperature dependence in the lower temperature range with an activation enthalpy of about 50 kJ/mol. The resemblance of these properties of the faster relaxation to the primitive relaxation of water in aqueous mixtures suggests that it is the primitive or JG β-relaxation of water confined in

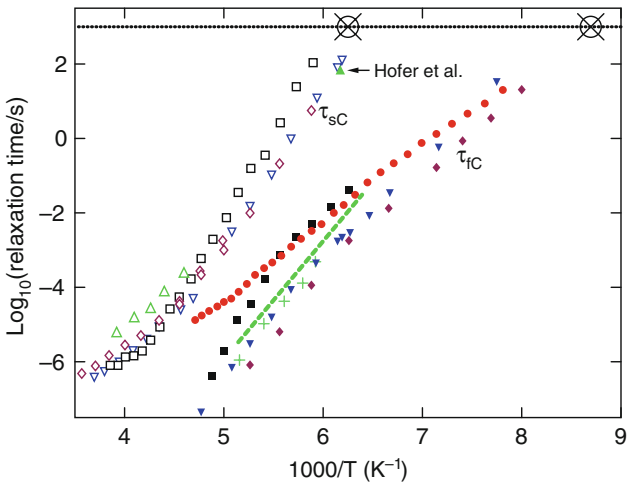

Fig. 2 Color online. τ_{sC} (*open diamonds*, and *open inverted triangles* for dry samples) and τ_{fC} (*closed diamonds*, and *closed inverted triangles* for dry samples), of a slower and faster relaxation of water confined in aged silica hydrogels [19]. τ_{fC} has Arrhenius T-dependence in the lower temperature range (activation enthalpy ≈ 50 kJ/mol). Comparison with τ_{sMS} (*open squares*) and τ_{fMS} (*closed squares*), of the slower and faster relaxations of water confined in molecular sieves with diameter of 10 Å [8]; τ_{JG} (*closed circles*) of 6 Å thick layer of water in Na-vermiculite clay [9]; τ_α or τ_{sPJ} (*open triangles*) and τ_{JG} or τ_{fPJ} (*dashed line*) of mixtures of 38.6 wt% of water with PHEMA [20, 21]; τ_α (*closed triangle*) of 34 and 42% of water with PHEMA [DSC from Hofer et al. 22, 23]; τ_{JG} or τ_{fPJ} (+) of mixtures of 50 wt% of water with PHEMA [20, 21]. The two ⊗ are relaxation times of two processes both equal to 10^3 s detected by adiabatic calorimetry at $T = 115$ and 160 K for water in the pores of silica gel with average diameter of 1.1 nm [16]

[1] We are not interested in the peaks of enthalpy release and absorption rates observed at 210 K of water confined in 1.8 nm diameter pores of MCM-41, and is attributed to glass transition of bulk water by Oguni et al. [18].

hydrogels. The slower relaxation has VFTH temperature dependence for its relaxation time, τ_{sC}, similar to that of typical α-process. It was suggested [19] that this relaxation originates from water molecules within the pores, which do not interact strongly with the matrix and behave collectively. Another possibility is interaction of water with silica, leading to silica being modified by hydrolysis. Whichever is the ultimate interpretation of the slower relaxation, it is an α-relaxation, and the faster relaxation with Arrhenius temperature dependence may be its JG β-relaxation. Their relaxation times, τ_{sC} and τ_{fC}, may be related by the CM Eq. 1 just similar to the relation between τ_{sMS} and τ_{fMS} of water confined in a molecular sieve shown in the previous Fig. 1. In fact, when we compare τ_{sC} with τ_{sMS}, and τ_{fC} with τ_{fMS} in Fig. 2, the values of each pair are similar, indicating that the origins of the fast process as well as the slow process are similar in the two cases.

We consider here also the relaxation of water confined in a hydrogel of PHEMA studied by Pathmanathan and Johari (PJ) [20, 21]. Within the experimental frequency ranging from 10 to 10^5 Hz, again, there are two relaxation processes. The faster relaxation of the 38.6 wt% water has Arrhenius temperature dependence for it relaxation time, τ_{fPJ}, with activation energy of 60.8 kJ/mol, as shown in Fig. 2 by the Arrhenius fit to the data (dashed line), but the data are not shown to avoid crowding. It can be seen from this figure that the relaxation times τ_{fPJ} are near τ_{fC} of the faster process found in water confined in aged silica hydrogels as well as τ_{fMS} of water confined in a molecular sieve. This coincidence suggests that τ_{fPJ} is the JG-relaxation time of water in the PHEMA hydrogel. The slower process of water in PHEMA hydrogels can only be observed at higher temperatures dielectrically. At lower temperatures, the d.c. conductivity dominates and preempts the observation of the slow process. Its relaxation time, τ_{sPJ}, determined from the dielectric loss spectra at several temperatures are shown as open triangles in Fig. 2. Again, at the same temperature, τ_{sPJ} is about the same as τ_{sC} or τ_{sMS}.

Calorimetric measurements of H_2O and D_2O in hydrogels of PHEMA performed by Hofer et al. [22, 23] show that water has very weak endothermic steps at 132 ± 4 K and at 162 ± 2 K for H_2O and 165 ± 2 K (D_2O), all for a heating rate of 30 K/min. The lower temperature, 132 ± 4 K, is nearly the same as T_g of hyperquenched glassy water [24–26]. The activation energy of the α-relaxation of hyperquenched glassy water is about 55 kJ/mol, which is also not far from 60.8 kJ/mol for τ_{fPJ}. Moreover, from the calorimetric data, Pathmanathan and Johari deduced that $\tau_{fPJ} = 53$ s at 135 K. The larger endothermic step at 162 K at the heating rate of 30 K/min indicates that the relaxation time of the slower process, τ_{sPJ}, is also 53 s at 162 K. This result, shown by a lone closed triangle located at $1000/T = 6.17$ in Fig. 2 and indicated there that it comes from Hofer et al., seems to be the continuation of τ_{sPJ} obtained by dielectric measurements at higher temperatures, as could be suggested by drawing a line to connect them. It can be seen by inspection of Fig. 2, τ_{sPJ}, τ_{sMS}, and τ_{sC} all have comparable values over the same temperature region where they increase toward long time-scale of vitrification. The activation enthalpy of τ_{sPJ} from calorimetric relaxation near 162 K is about 120 kJ/mol or twice the activation energy of τ_{fPJ}. From the contrasting properties of τ_{sPJ} and τ_{fPJ} discussed above, we suggest in PHEMA hydrogels that the slower process is the relaxation of water interacting with PHEMA, similar to water interacting with the inner surface of molecular sieves [8] or with the silica in silica hydrogels [19]. The faster process could be considered as the JG β-relaxation of water in PHEMA hydrogels. Again τ_{sPJ} and τ_{fPJ} are related by an analog of the CM Eq. 1, and there is a change of the T-dependence of τ_{fPJ} at the temperature where τ_{sPJ} reaches the long time of 10^3 s similar to that found for other mixtures (see Figs. 1–3).

Study of water confined in the pores of silica gel with average diameter of 1.1 nm by adiabatic calorimetry reported again the occurrences of a faster and a slower

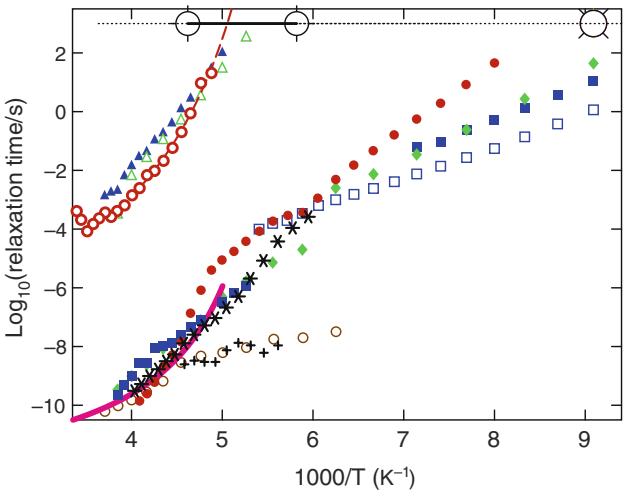

Fig. 3 Color online. τ_W (*squares* and *diamonds*) and τ_{BSA} (*triangles*) in 20 and 40% (w/w) solution of bovine serum albumin (BSA) in water [27]. The two *large circles* joined by a *line* indicate the temperature range of the α process of hydrated BSA and the *large circle* with four spokes is the water JG β-relaxation observed by adiabatic calorimetry [29]. τ_W (*red closed circles*) and τ_{Mb} (*red open circles*) in water/glycerol solution of myoglobin [28]. *The magenta solid line*: VFTH fit to the relaxation time, τ_c, of reorientational motion of heavy water (D_2O) in D_2O-hydrated myoglobin (0.35 g/g) from deuteron NMR [30, 31]. The slower and faster dielectric relaxation times of hydrated lysozyme [35], τ_{1K} (*) and τ_{2K} (+). Translational relaxation time, $\langle\tau_T\rangle$, for the hydration water in lysozyme from [34] (*brown open circles*) show change from VFTH T-dependence above $T_L = 220$ K to Arrhenius T-dependence below T_L. Note the good agreement of τ_{2K} with $\langle\tau_T\rangle$ below T_L, and τ_{1K} with $\langle\tau_T\rangle$ above T_L

process [16]. We do not discuss the data of water confined in 6-, 12- and 52-nm pores of silica gel in [16] because of reported large fraction of ice formed in the central portion of these pores, which could have complicated the observed results. The relaxation times of the two processes both equal to 10^3 s were detected by adiabatic calorimetry at $T = 115$ and 160 K. They are shown by the two larger circles (⊗) at the top in Fig. 2. The relaxation times of the slower process are coincident with the values of τ_{sC}, and τ_{sMS} when they are extrapolated to lower temperatures. The relaxation times of the faster process agree approximately with τ_{fPJ}, τ_{fC}, and $\tau_{6Å}$ (as well as τ_{JG} of the 50% water mixtures with PVME) when their Arrhenius dependences are extrapolated down to 115 K. Again, the Arrhenius activation enthalpies of all these processes are about the same. Thus, the two processes of water confined in 1.1-nm pores of silica gel observed by adiabatic calorimetry have to be interpreted in the same way. In particular, the faster one is an intrinsic primitive relaxation of water, independent of the form of confinement or mixtures.

Dynamics of hydrated proteins

Water is important for biological systems to function. Dehydrated proteins cannot function, but a thin layer of water in the hydration shell hydrogen bonded to the protein fully activates the functionality. The water in the hydration shell is an intrinsic part of the protein structure, as opposed to the bulk water outside. Among several interesting aspects, perhaps the most often addressed one is the role played by water in determining the dynamic properties and function. Recently, broadband dielectric measurements have been made on a sample containing an equal mass fraction of myoglobin, water, and glycerol by Swenson et al. [27], and 20 and 40% (w/w) solution of bovine serum albumin (BSA) in water by Shinyashiki et al. [28]. Excluding the relaxation of ice formed in the bulk water, d.c. conductivity and other processes that are irrelevant for the present discussion, two major relaxation processes originating from water in the hydration shell and the hydrated myoglobin or BSA are observed. Their relaxation times determined from fits to the isothermal data of $\varepsilon^*(\nu)$ (not shown) are plotted against reciprocal temperature in Fig. 3. The loss peak of water in the hydration shell of the 20 wt% BSA–water mixture at lower temperatures seems to be composed of two processes close to each other, and their relaxation times are represented by open and closed blue squares. A single process is obtained for the 40 wt% BSA–water mixture and shown by green closed diamonds. All these relaxation times of water in the hydration shell, collectively denoted by τ_W, have Arrhenius T-dependence from 100 K and up to about 200 K. Above 200 K, the relaxation times of water in the hydration shell are represented by blue open circles and closed diamonds for the 20 and 40% (w/w) BSA–water mixtures, respectively. It can be seen that the Arrhenius T-dependence of τ_W at temperatures below about 200 K is replaced by a stronger and non-Arrhenius T-dependence after crossing some temperature in the neighborhood of 200 K. The gap between τ_W in this neighborhood is the artifact of fitting isothermal data by Cole–Cole functions, and should not be there. The relaxation times of the hydrated BSA, τ_{BSA}, are shown by the blue closed triangles and green open triangles for the 20 and 40% (w/w) BSA–water mixtures, respectively. With the much stronger T-dependence, τ_{BSA} reaches the range of 10^2–10^3 s near 200 K, suggesting that it is the structural α-relaxation and that the glass transition of the hydrated BSA occurs at some temperature $T_{gBSA} \approx 200$ K. This happening is supported by heat capacity and enthalpy relaxation rate measurements of a 20% (w/w) BSA–water mixture by Kawai et al. [29]. These authors have found several enthalpy relaxations with relaxation time of 10^3 s originating from different processes. The one found in the broad range from 170 to 220 K are indicated by the thick line at 10^3 s bounded on both sides by ⊗ in Fig. 3. It can be seen from the figure that the dielectric τ_{BSA} falls within the temperatures range of enthalpy relaxation. Kawai et al. found another enthalpy relaxation with relaxation time of 10^3 s in the temperature range from 100 to 120 and centered at 110 K (indicated by ⊕). This temperature is in rough agreement with the dielectric, τ_W, when extrapolated to 10^3 s, proving that adiabatic calorimetry and dielectric relaxation show the same water relaxation. Almost the same enthalpy relaxation was found for water confined within 1.1-, 1.6- and 1.8-nm nano-pores of silica MCM-41 [18] and of silica gels [16]. The τ_W of water in the hydration shell at temperature below T_{gBSA} is comparable in magnitude and activation energy to the dielectric JG relaxation of water in hydrophilic mixtures [1] and nano-confined water [8, 11, 19–23]. This suggests that τ_W is truly the primitive or JG relaxation of water in the hydration shell. The change of the T-dependence of τ_W at T_{gBSA} is the same as that found in the JG relaxation of water in other aqueous mixtures [1], nano-confined water, and a component in mixtures of two van der Waals glassformers [1]. This general relation between the JG β-relaxation and the α-relaxation has been explained by the CM [2–7].

The relaxation times, τ_W and τ_{Mb}, of the JG relaxation of water and the α-relaxation of hydrated myoglobin, respectively, from Swenson et al. [27] are reproduced (red open and closed circles) in Fig. 3 to compare with those of the hydrated BSA. Again, the JG relaxation time, τ_W, of water in the water/glycerol solvent of myoglobin is similar to what we find in hydrated BSA, and there is a change of the T-dependence of its relaxation time at the glass

transition temperature of the hydrated myoglobin, τ_{Mb}, which is also near 200 K. In the glassy state, the relaxation times of JG relaxation of water in the water/glycerol solvent of myoglobin are longer and have larger activation energy than pure water in hydrated BSA. This is understandable because glycerol is less mobile than water.

Also shown in Fig. 3 is the relaxation time, τ_c, of reorientational motion of heavy water (D_2O) near the surface of myoglobin in D_2O-hydrated myoglobin (0.35 g/g) determined by deuteron NMR [30]. The method probes the reorientational relaxation of the O–D vector, and τ_c obtained from about 200 to 300 K has been fitted by the VFTH T-dependence, $\tau_c(T) = (0.96)\exp[460/(T - 167)]$ ps, given in [31] and shown here in Fig. 3 by the solid magenta line. Good agreement between τ_c from NMR and τ_W from dielectric measurements can be seen. According to our interpretation similar to those in other non-aqueous [2–6] and aqueous mixtures [1] and nano-confined water, τ_W is the JG relaxation time of water which is not undergoing glass transition at 200 K itself, but is the precursor of the glass transition of the hydrated protein at near 200 K. In fact, the dielectric τ_W reaches 10^3 s near 110 K in the case of hydrated myoglobin, and at about 100 K in the case of the hydrated BSA which is near 110 K, the glass transition temperature of hydration water from calorimetry [29]. The difference of our interpretation from that offered by Doster and Settles on their τ_c from NMR is brought out by quoting the statement they made [30]: "The structural relaxation time related to translation of hydration water varies however in a super-Arrhenius manner with temperature as the neutron scattering and the deuteron relaxation data demonstrate. These results provide evidence that hydration water turns into a glassy state near 200 K." The same kinetic glass transition of the solvent near the protein surface coupled to the protein motions was used earlier in the interpretation of the "dynamic transition," i.e., rapid increase of the mean square displacement of hydrated protein motion past 200 K seen by Mössbauer effect [32] and neutron scattering [33].

Chen et al. [34] used quasielastic neutron scattering and analyzed the data using the relaxing cage model, to determine the average translational relaxation time, $\langle\tau_T\rangle$, for the hydration water in lysozyme. They found that $\langle\tau_T\rangle$ follows a VFTH T-dependence above $T_L = 220$ K, but changes abruptly to have the Arrhenius T-dependence with activation energy of 3.13 kcal/mol, as shown by brown open circles in the lower left part of Fig. 3. Just similar to the observation of nano-confined water made by the same group [12, 13], this behavior of $\langle\tau_T\rangle$ is interpreted as fragile-to-strong liquid–liquid transition involving the structural α-relaxation of the hydration water. It can be seen by inspection of Fig. 3, above $T_L = 220$ K where $\langle\tau_T\rangle$ follows the VFTH T-dependence of "fragile" water, there is good agreement between $\langle\tau_T\rangle$ of hydration water in lysozyme with the dielectric JG relaxation time, τ_W, of hydration water in myoglobin [27] or in BSA [28], as also with the reorientational time, τ_c, of heavy water (D_2O) near the surface of myoglobin in D_2O-hydrated myoglobin determined by deuteron NMR [30]. Such agreement suggests, that above $T_L = 220$ K, $\langle\tau_T\rangle$ is actually the primitive or JG relaxation time of hydration water. However, neither τ_W nor τ_c exhibits the abrupt change to the Arrhenius T-dependence below 220 K as Chen et al. found for $\langle\tau_T\rangle$. Extrapolating the Arrhenius T-dependence of $\langle\tau_T\rangle$ below $T_L = 220$ K given by Chen et al. to low temperatures, we find roughly 47 K would be the glass transition temperature for the "strong" water defined by $\langle\tau_T\rangle = 10^3$ s. This low value of T_g for hydration water is unrealistic, and shows once more that Chen et al. did not observe the α-relaxation of hydration water below $T_L = 220$ K.

The results of a recently published dielectric relaxation study of lysozyme hydrated to a level of $h = 0.4$ g water per gram of protein by Khodadadi et al. [35, 36] may have helped to unravel the mystery of the identity of the "strong" water having Arrhenius T-dependence of $\langle\tau_T\rangle$ below $T_L = 220$ K. In the isothermal spectrum at temperatures between 203 and 223 K, one major loss peak shows up but, in addition, there is a faster process on its high frequency flank with much weaker relaxation strength. The spectra in this temperatures range were fitted by the sum of two Cole–Cole distribution functions, and the relaxation times of the slower and major process, τ_{1K}, and the faster and minor process, τ_{2K}, determined. At temperatures above 223 K, the spectra show only the major loss peak and were fitted with a single Cole–Cole distribution function. The results presented in Fig. 3 show that τ_{1K} (black asterisks) of hydration water in lysozyme is not too different from τ_w of hydration water in BSA or in myoglobin, or τ_c of heavy water (D_2O) in myoglobin from deuteron NMR for temperatures down to about 167 K. Moreover, τ_{1K} is approximately the same as $\langle\tau_T\rangle$ of Chen et al. above $T_L = 220$ K, but in contrast to $\langle\tau_T\rangle$, it continues to be present at temperatures below 220 K. Remarkably, τ_{2K} of the faster and minor (shown by + sign) has about the same value and small activation energy as $\langle\tau_T\rangle$ of Chen et al. below $T_L = 220$ K. This correspondence was also pointed out by Khodadadi et al. [36]. The comparison with the dielectric data suggests that quasielastic neutron scattering method and analysis used by Chen et al. could be more sensitive to the faster minor process having relaxation time $\langle\tau_T\rangle \approx \tau_{2K}$ at lower temperatures. Owing to this, Chen et al. possibly missed detecting the slower major process below $T_L = 220$ K, resulting in the abrupt change of temperature dependence of $\langle\tau_T\rangle$ from the non-Arrhenius form of τ_{1K} to the Arrhenius one of τ_{2K}. Hence, there is no fragile-to-strong dynamic crossover of hydration water at $T_L = 220$ K.

In addition to dielectric relaxation, Khodadadi et al. [35, 36] studied the dynamics of lysozyme hydrated in D_2O using quasielastic neutron scattering. The neutron scattering data were cast in terms of the imaginary part of the susceptibility, $\chi''(Q,v)$, where Q is the scattering vector and v the frequency, and the characteristic relaxation times from its peak frequency. There is only one peak in $\chi''(Q,v)$ and its relaxation time, $\tau_{n\mathrm{K}}$, is almost the same as $\tau_{1\mathrm{K}}$ over the temperature range from 200 to 295 K, and also comparable to τ_{w} of hydration water in BSA or in myoglobin, or τ_c of heavy water (D_2O) in myoglobin. Since neutrons scatter mostly from hydrogen atoms, the neutron scattering spectra of the lysozyme/D_2O sample reflect the motion of the protein and not the deuterated water of hydration. However, this observed protein motion is *not* the structural α-relaxation of the hydrated lysozyme. This is because we have learned from the dielectric data of hydrated myoglobin [27] and hydrated BSA [28] that the structural α-relaxation of hydrated proteins is a separate entity with relaxation time different from τ_{w} or τ_{c}, and has a T_g of its own determined at 10^3 s by adiabatic calorimetry (see Fig. 3). Furthermore, $\tau_{1\mathrm{K}}$ and $\tau_{n\mathrm{K}}$ are comparable to τ_{w} or τ_{c}, indicating that the former like the latter are the JG β-relaxation times and not the structural relation times of the hydrated protein. Altogether, these facts cannot be reconciled with the assignment of the motion with relaxation time $\tau_{1\mathrm{K}}$ or $\tau_{n\mathrm{K}}$ to "structural relaxation of the protein" in [35], or "protein's structural relaxation coupled to hydration water" in [36] by Khodadadi et al.

Study of the dependence of the dielectric $\tau_{1\mathrm{K}}$ on hydration level h [36] found that $\tau_{1\mathrm{K}}$ increases with decreasing h. Six orders of magnitude increase of $\tau_{1\mathrm{K}}$ was observed when h is decreased from 0.37 to 0.05. This property is found also in the primitive or JG β-relaxation time of water, τ_{JG}, in aqueous mixtures on decreasing the water content [1]. An example can be taken from mixtures of glycerol with water. The large increase of τ_{JG} with decreasing water content can be seen in Fig. 5 in [1]. The hydrated lysozyme dielectric data of Khodadadi et al. [36] at any h were not taken over wide enough range of temperature. Otherwise, they should see that the temperature dependence of $\tau_{1\mathrm{K}}$ changes from VFTH law to the Arrhenius law at T_g of the hydrated protein, and the similarity of results to the glycerol/water mixture would be more complete.

In the previous section on dynamics of aqueous mixtures, we have already mentioned that the two components are coupled together in all motions because of hydrogen bonding of water to the hydrophilic solute. The same applies to hydrated protein where the dynamics of water and protein are coupled. Evidence of coupled dynamics comes from molecular dynamics simulations of the globular protein Ribonuclease A done by Tarek and Tobias [37], which show that the anharmonic and diffusive motions involved in the protein structural relaxation are correlated with the protein–water hydrogen bond dynamics, and also that the complete structural relaxation of the protein requires relaxation of the hydrogen bond network via solvent translational displacement. Experimental studies showing evidences that the dynamics of protein and solvent are physically coupled can be found in the review by Ringe and Petsko [38]. Here, we cite just a few [39, 40]. Consequently, the primary relaxation as well as the secondary relaxation in hydrated proteins involves some motions of both the hydration water and the protein, and the same relaxation is probed by technique exclusively sensitive to the protein or to the water. This explains why Khodadadi et al. [35, 36] found similar neutron and dielectric relaxation times and spectra even though neutron scattering probes exclusively the lysozyme, and not the deuterated hydration water. The same explains the similar temperature dependences of the mean square displacements $\langle x^2(T)\rangle$ of hydrogen atoms obtained by neutron scattering, regardless of whether the hydrogen atoms are from the protein (hydrated in D_2O) or from H_2O of the hydration water [31, 41]. We have used the terms: (1) primitive or JG β-relaxation of hydration water, and (2) structural α-relaxation of the hydrated protein. Although these terms seem to imply that only one component is involved in each process, participation of the other component must be borne in mind because of coupling of hydration water and protein by hydrogen bonding.

The mean-square-displacements $\langle x^2(T)\rangle$ of all hydrated proteins before from neutron scattering [30, 31] and Mössbauer spectroscopy [32] show a change from weak T-dependence at low temperatures to a much stronger dependence at some temperature within the range of 200–230 K. Interest in this so-called "dynamic transition" originates from the fact that onset of biochemical activity of proteins is also at about the same temperature. Various explanations of this property of $\langle x^2(T)\rangle$ have been offered in the past [31, 41, 42]. Chen et al. [34] obtained the mean-squared atomic displacement of the hydrogen atoms, $\langle x^2\rangle$, of hydrated lysozyme as a function of T and found the crossover in its T-dependence at about 200 K. This was interpreted by Chen et al. as due to fragile-to-strong crossover of hydration water at $T_L = 220$ K. As discussed above, the fragile-to-strong crossover may be an artifact of neutron scattering and data analysis, and, hence, it is not valid explanation of the "dynamic transition". Based on their own data, Khodadadi et al. [36] proposed an explanation entirely different from all others. They believed that the "dynamic transition" is caused by $\tau_{n\mathrm{K}}$ (what they called the protein's structural relaxation time) on entering the resolution window of the neutron spectrometer in the temperature range of the "dynamic transition", and is not due to some feature of the protein dynamics. A critique of this

explanation can be drawn from the results of the mean-square-displacements $\langle x^2(T)\rangle$ of ordinary glass-formers from quasielastic neutron scattering experiments as performed on hydrated proteins. Change of T-dependence of $\langle x^2\rangle$ similar to the "dynamic transition" of hydrated proteins has been seen in various kinds of glass-formers always at the glass transition temperature, T_g, and independent of the resolution window of the neutron spectrometer used [43, 44]. Neutron spectrometers, IN10, IN13, and IN6, of the Institute Laue-Langevin have energy resolutions (FWHM) of 1 μeV, 8 μeV, and 0.2 meV, respectively. The data obtained by any of these spectrometers with different resolutions show that the crossover is invariably at T_g of the glass-former. The remarkable fact, that the crossover temperature is always T_g, has been considered to be one of the important and general phenomena of glass transition [45]. Unless the mean-square-displacements $\langle x^2(T)\rangle$ of hydrated neutron measured by neutron scattering are totally different from that of ordinary glass-formers in origin, the above facts cast doubt on the validity of explaining the "dynamic transition" by the structural relaxation time entering the resolution window of the neutron spectrometer [36]. For ordinary glass-formers, the structural relaxation time at T_g of ordinary glass-formers is ten or more orders of magnitude longer than the resolution window of neutron spectrometers and cannot be involved in the measured $\langle x^2(T)\rangle$.

Only much faster relaxation processes than the structural relaxation are probed when measuring the neutron $\langle x^2(T)\rangle$, and are responsible for the observed crossover at T_g. Near T_g and at times shorter than nanoseconds of neutron and light scattering experiments, molecular units are caged and thus the fast relaxation comes from caged molecule dynamics (excluding contribution from local intramolecular motions such as methyl group if present). An explanation for the crossover in T-dependence of $\langle x^2(T)\rangle$ observed in ordinary glass-formers was given in [46] as due to the change of the T-dependence of the caged molecules dynamics contributing to $\langle x^2\rangle$ on crossing T_g. In the neutron or light scattering susceptibility spectra $\chi''(\nu)$, the caged molecule dynamics show up as the nearly constant loss (NCL), i.e., $\chi''(\nu) = p\nu^{-c}$ with $0 < c \ll 1$ [43–50], which is the equivalent of $\langle x^2(t)\rangle$ having time dependence proportional to t^c. Similar to $\langle x^2(T)\rangle$ from elastic incoherent neutron scattering, the intensity of the NCL changes from a weak T-dependence below T_g to a stronger T-dependence above T_g. An example is the light scattering spectra of PIB (see Fig. 3 in [48] or Fig. 10 in [50]). The change of T-dependence of the NCL or $\langle x^2(T)\rangle$ across T_g was shown [48] to be driven by the observed change of the JG β-relaxation time from the Arrhenius dependence below T_g to a stronger one above T_g [1–7]. We explain the "dynamic transition" of $\langle x^2\rangle$ for hydrated proteins originating from caged molecular dynamics as well as the JG relaxation of water entering the time window of the neutron scattering spectrometer in the same way as for ordinary glass-formers [48]. This explanation is satisfactory because τ_W of hydrated BSA [28] and hydrated myoglobin [27] as well as $\tau_{n\mathrm{K}}$ and $\tau_{1\mathrm{K}}$ of hydrated lysozyme [36] have been identified as the JG β-relaxation times of hydration water in these proteins, and τ_W also exhibits the change in T-dependence when crossing T_g in the "dynamic transition" range of 200–230 K. These are demonstrated by the dielectric and adiabatic calorimetry data of hydrated myoglobin or BSA in Fig. 3.

From the discussions based on the above experimental data on dynamics of hydrated proteins, we conclude that the adiabatic calorimetric measurements [29] are pivotal in proving that the two major relaxation processes, the primitive or JG β-relaxation of hydration water and the structural α-relaxation, are distinct, but yet connected. They are distinct because their relaxation times reach 10^3 s at vastly different temperatures, $T_{g\beta}$ for the β-relaxation and $T_{g\alpha}$ for the α-relaxation, as determined by adiabatic calorimetry. They are connected because of the observed change in the temperature dependence of the dielectric β-relaxation time when $T_{g\alpha}$ is crossed. These features are analogous to the dynamics found in many aqueous mixtures [1]. Moreover, in the Arrhenius temperature regime, the β-relaxation time of hydration water in protein is comparable in magnitude and has similar activation enthalpy as for the primitive or JG β-relaxation of many aqueous mixtures. There is also analogy with binary mixtures of van der Waals liquids [1–5], although the analogy is not total because in the absence of hydrogen bonding, each component has its own α- and JG β-relaxations. There are other connections between the primitive or JG β-relaxation and the α-relaxation in mixtures and in neat glass-formers [1–7, 51] beyond the one discussed here. These connections occur because the primitive relaxation is the precursor of the multi-body relaxation dynamics evolving with time until the α-relaxation is reached. The explanation has been given by the CM [1–7], and the same explanation applies to the dynamics of hydrated proteins.

On the contrary, without the benefit of considering the full spectrum of long-time adiabatic calorimetric and low-frequency dielectric data, the authors of neutron scattering [31, 35, 36] and deuteron NMR [30, 31] experiments probing short-time dynamics were led to draw contradictory conclusions and interpretations. Chen et al. [34] and Khodadadi et al. [35, 36] concluded that they have observed the structural α-relaxation of the hydrated protein. Doster and Settles [30] interpreted their deuteron NMR data as due to the structural relaxation related to translation of hydration water of myoglobin. However, as clearly demonstrated in Fig. 3, the neutron $\langle\tau_T\rangle$ above $T_L = 220$ K of Chen et al. [34], the neutron $\tau_{n\mathrm{K}}$ and dielectric $\tau_{1\mathrm{K}}$ of Khodadadi et al. [35, 36], as well as τ_c from deuteron NMR

of Doster and Settles are the β-relaxation times of hydration water at temperatures above $T_{g\alpha}$ unequivocally determined by adiabatic calorimetry in the case of hydrated BSA (see Fig. 3). The structural relaxation times of the hydrated BSA [28] and myoglobin [27] determined by dielectric relaxation spectroscopy have much longer times than $\langle\tau_T\rangle$, $\tau_{n\mathrm{K}}$, $\tau_{1\mathrm{K}}$, and τ_c from the other authors.

Lusceac et al. [52] reported studies of the dynamics of water in the hydration shell in hydrated collagen, elastin, and myoglobin by ^{2}H NMR. They made several incorrect statements on dynamics of hydration water. First, they claimed that the large-angle jump they observed at low temperatures is strong evidence against it being a Johari-Goldstein β-relaxation. This claim is based on the bold assumption that the motion of JG β-relaxation in all glassformers has to be exactly the same irrespective of chemical structure and bonding as the one Vogel found before for polybutadiene and toluene. Water is the smallest molecule in Nature that involves hydrogen bonding contrary to van der Waals glassformers. After the hydrogen bond is broken, there is no reason that local reorientation of the small water molecule has to be restricted to small angles. On the contrary, local motion in larger and carbon containing polybutadiene and toluene in the glassy state are more restricted by dense packing and steric constraints. Polybutadiene has, in addition, bonded interaction along the chain. Therefore, there is no compelling reason to assert that the amplitude of the motion of the JG β-relaxation of water (called water-specific β process by Lusceac et al. in [52]) in the hydrated shell has to be the same as that of the JG relaxation of polybutadiene and toluene, or even glycerol which has not only a hydrogen bonding but also a carbon backbone. Moreover, there is a similar ^{2}H NMR study of JG β-relaxation of neat polyalcohols, including glycerol, threitol, xylitol, and sorbitol [53]. Representing the spatially restricted motion of the JG βrelaxation in a cone, the semi-angle Θ of the cone for sorbitol deep in the glassy state is about three times larger than that of threitol. This example shows that the amplitudes of motion of JG β-relaxations are not necessarily the same for all glassformers, and definitely not water.

Second, they suggest the following picture of the temperature-dependent dynamics of protein hydration waters [52]. "Above about 220 K, water exhibits isotropic rotational motion, which is governed by pronounced dynamical heterogeneities with short lifetimes. Hence, the dynamics resembles the α process of supercooled liquids, although the vicinity of protein surfaces may lead to some differences …". "Below about 220 K, water exhibits anisotropic large-amplitude rotational motion, implying existence of a water-specific β process, which shows similar features for the hydration waters of various materials, including polymers and inorganic nanoporous matrices." For hydrated myoglobin [27, 54], lysozyme [39, 54] and hydrated BSA [28, 29, 54–56], a slower α process involving the protein coupled with hydration water has already been detected by dielectric spectroscopy [27, 28, 55, 56], adiabatic calorimetry [29, 39], and mechanical spectroscopy [54] (see Fig. 3). This slow α process is responsible for the glass transition temperature, T_g, not far from 220 K for hydrated myoglobin and BSA, and, hence, its relaxation time at 220 K is very long. On the contrary, the other α process of hydration water suggested by Lusceac et al. [52] has much shorter relaxation time of about 10^{-7} s at 220 K. If we accept the interpretation of Lusceac et al., then two α processes are present in the hydration shell. As commonly believed, the hydration shell consists of two or three layers of water, and, hence, the presence of these two disparately different α processes associated with water in it is highly unlikely. Since Lusceac et al. invoke similarity to aqueous mixtures, it is worth pointing out that the dielectric strength of the water-specific process increases with increasing temperature above T_g, which is a characteristic of secondary relaxation and not that of α process [1].

The term, JG β-relaxation, is merely used to distinguish a special class of secondary relaxation that is the true precursor of the structural α-relaxation. Lusceac et al. seem to have misinterpreted the term as if its character has to be the same both above and below T_g. In fact, they used the isotropic motion of hydration water at high temperatures as another indication that it is not the JG relaxation above T_g. Actually, the more exact term to replace JG relaxation in our interpretation of water-specific process is the primitive relaxation of the CM, and it must become isotropic above T_g so that it can be the precursor of the isotropic α-relaxation as found in hydrated myoglobin. For hydrated elastin and collagen, both NMR and dielectric relaxation [57] found a secondary relaxation with Arrhenius T-dependence for its relaxation time, τ_β, at all temperatures below $T_g = 275$ K with activation energy of 53 kJ/mol corresponding to the energy needed to break two hydrogen bonds. The characteristics of τ_β is similar in every respect to what we found and called the JG relaxation in hydration water of proteins [28, 55, 56], various aqueous mixtures, and nano-confined water [1]. After breaking two hydrogen bonds, as suggested by the activation energy $\approx$ 53 kJ/mol of the JG relaxation of hydration water, the water molecule is free to rotate and translate. This combined rotational and translational freedom of the JG relaxation of water can rationalize that its ^{2}H NMR line-shape was observed as a Lorentzian at temperatures down to about 220 K in hydrated elastin and collagen. The anisotropy of the NMR interaction is averaged out by the presence of the translational motion, rendering the rotational motion of water isotropic, rather than anisotropic. At lower temperatures

where τ_β becomes long compared to 10^{-7} s, translational motion is limited, and anisotropic motion is observed. For hydrated myoglobin, translation diffusion of water was actually observed above T_g, and explains why water exhibits isotropic rotational motion.

JG β-relaxation or confined relaxation of the lower T_g component in binary mixtures of two glass-formers?

We present one more example in which thermal analysis and adiabatic calorimetry play the decisive role in settling the controversy in the dynamics of the lower T_g component in binary mixtures of two glass-formers. Lorthioir, Alegria and Colmenero (LAC) [58], and Cangiolosi, Alegria, Colmenero (CAC) [59] considered binary mixtures of two components with large difference in their T_gs in the pure states, and rich in the high T_g component (h). They proposed that the minority and lower T_g component (l) will be "confined" in the frozen matrix of the majority component at temperature below its glass temperature in the mixture, T_{gh}, where the α-relaxation time of the majority component, τ_{ah}, is very long. The consequence of confinement according to LAC is that the minority component can only execute localized motion within the frozen matrix of the majority component. For the PVME/PS blends with concentrations of PS higher than 50 wt%, the PVME relaxation with Arrhenius T-dependence for its relaxation time at temperatures significantly lower than T_{gh} was found [58]. They called this α'-relaxation, and used it to support the existence of "localized, weakly cooperative PVME motions resulting from the topological constraints imposed by the frozen PS chains." Also observed are two very fast secondary relaxations of PVME. They originate from the restricted rotational motions of the methyl ether group in PVME, and the free rotational motions of PVME side chains [60]. Hence, they are intramolecular secondary relaxations, and according to the criteria of Ngai and Paluch [7], they are not the JG β-relaxation of PVME in either the neat state or the blends. The JG β-relaxation of neat PVME is not resolved by dielectric measurements.

In addition to the α'-relaxation, LAC also observed the α-relaxation of PVME in blends with 35, 50, 70, and 80% PS isochronically at 1 Hz, and also isothermally within the frequency window of $10^{-1} < \nu < 10^6$ Hz at temperatures higher than 280 K. It becomes very broad at 70 and 80% PS. Miwa et al. reported two T_gs, one associated with the PVME component and other with the PS components from temperature-modulated DSC measurements for PS/PVME blends [61]. The situation of PVME/PS blends are, thus, similar to that found in mixtures of picoline, *tert*-butylpyridine, or quinaldine with tristyrene or polystyrene, where the JG β-relaxation of these rigid polar molecules are not resolved in the pure state, but becomes resolved on mixing with tristyrene or polystyrene, and are seen together with the cooperative α-relaxation of the rigid polar molecules. It is also similar to that found by dielectric relaxation as well on a series of poly(*n*-butyl methacrylate-*stat*-styrene) copolymers with styrene contents ranging from 0 to 66 mol% [62, 63]. At 0% styrene, poly(*n*-butyl methacrylate) has its JG β-relaxation close to the α-relaxation and barely resolved. However, with increasing styrene content, the separation between the two relaxations increases and both relaxations are present in all the copolymers. By analogy, we would identify this so-called α'-relaxation PVME relaxation with Arrhenius T-dependence for its relaxation time, τ'_α, as the resolved JG β-relaxation (or the primitive relaxation of the CM) of PVME in the mixtures, but unresolved in neat PVME. If consideration is limited to the α'-relaxation, then the difference between our interpretations of its origin and those by LAC can be regarded as a matter of semantics because it is a local and non-cooperative relaxation in both interpretations. However, there are some major differences that can differentiate the two interpretations for verity, and should not be missed.

First, it is important to point out that the α'-relaxation in 80% PS blend is not only observed below 280 K where τ'_α is Arrhenius, but at much higher temperatures, and τ'_α is no longer Arrhenius. It shows up as a prominent loss peak at 10^6 Hz when $T = 328$ K (see Fig. 5 of LAC), and certainly it will continue to higher frequencies on further increase of temperature. For $T \geq 280$ K, LAC already conceded that the α-relaxation of PVME appears over a broad frequency range at temperatures from 280 to 328 K in isothermal loss spectra obtained within the frequency window of $10^{-1} < \nu < 10^6$ Hz. It also appears as a broad loss with an apparent inflection at about 290 K in the isochronal spectrum at 1 Hz. This α-relaxation of PVME will certainly continue to be present at temperatures below 280 K, although it is not detected by the dielectric spectroscopy LAC used because of the low frequency cut-off at 10^{-1} Hz. Concerning the α'-relaxation in 80% PS blend, from the plot of log(relaxation time) versus 1000/T in Fig. 7 of LAC, one can see that there are data points of $\log_{10}[(\tau'_\alpha\ (\mathrm{s})]$ shown not only above $(1000/T) = 3.57\ \mathrm{K}^{-1}$ corresponding to $T \leq 80$ K, but also for $(1000/T)$ down to about $3.23\ \mathrm{K}^{-1}$, which corresponds to $280 \leq T < 310$ K. Therefore, although separated by many decades of time, both the α-relaxation and the α'-relaxation are observed at the *same* temperature when it is sufficiently above 280 K or the glass transition temperature T_{gl} of the PVME component. LAC proposed that PVME is confined in environments consisting of ''frozen'' PS chains in the 80% PS blend, and its segmental motion can only give rise to the local α'-relaxation, and nothing else. Clearly, this is contradicted by the coexistence of the cooperative α-relaxation and the

α'-relaxation at the *same* temperature when it is above or below T_{gl}, and both relaxations originate from the PVME component.

The existence of the α-relaxation of the lower T_g component (l) at temperatures below T_{gh} and above T_{gl} is a common occurrence in miscible polymer blends. It is by now well known in various miscible polymer blends that separate and different structural α-relaxation of the two components can be observed experimentally by ^{3}C MAS NMR [64], combination of mechanical and dielectric spectroscopies [65, 66], by deuterium NMR measurements [67], and by calorimetry [61, 68, 69]. For a review and more examples, see [70]. The α-relaxation of the lower T_g component (l) with VFTH temperature dependence has been observed at temperatures below T_{gh} and above T_{gl}. The example closely related to the PVME/PS blends of LAC is the dielectric relaxation study of poly(vinyl methyl ether) (PVME)/poly(2-chlorostyrene) (P2CS) blends [60, 71]. P2CS has a higher T_g than PS. In the 30%PVME/70%P2CS blend, two separate cooperative segmental α-relaxations of the PVME and the P2CS components were found in the isochronal spectrum. Extreme examples are the PEO/PMMA blends which have very large difference between T_{gh} of PMMA and T_{gl} of PEO (poly(ethylene oxide)). Nevertheless, deuterium NMR study of blends of deuterated PEO with PMMA [72, 73] found that the segmental α-relaxation of PEO in any of the blends with 3, 6, 10, and 20% PEO was many orders of magnitude faster than the dynamics of PMMA at the T_{gh} of PMMA. The T-dependence of the segmental α-relaxation time of PEO, $\tau_{\alpha l}$, is not Arrhenius. For the 3% PEO blend, $T_{gh} = 391$ K, and the α-relaxation time of PEO is found by deuteron NMR down to 285 K, more than 100 degrees below T_{gh}. The observation contradicts LAC idea that the 3% PEO will be confined by the frozen PMMA, and segmental motion of PEO can only give rise to the local and Arrhenius α'-relaxation. Just as in the PVME/PS blends, a non-JG γ-relaxation plus a JG β-relaxation [74] were found by Runt and co-workers in amorphous 20%PEO/80%PMMA blend [75]. Differential scanning calorimetry measurement of blends of a low molar mass PEO ($M_n = 300$ g/mol), and a PMMA ($M_n =$ 10,000 g/mol) found that blends with 25% PEO have two broad but distinctly different glass transitions in the range $-64 < T < -8$ °C with an average of -36 °C for the PEO component, and $55 < T < 106$ °C with an average of 81 °C for the PMMA component [69]. Thus, the cooperative α-relaxation originating from the PEO component was still observed in DSC at $T_{gl} = -36$ °C, more than 100° below $T_{gh} = 81$ °C of the PMMA component.

Returning to the 20%PEO/80%PMMA blend data of LAC, τ'_α has the Arrhenius dependence only at temperatures below approximately 290 K. Above 290 K, τ'_α exhibits a stronger T-dependence. Owing to the very broad α-loss peak of the PVME component in either the isochronal or the isothermal spectra, no exact value of T_{gl} can be given, but 290 K is possibly a candidate for T_{gl}. If so, the observed change of T-dependence of τ'_α when crossing 290 K is the same as that found in the mixtures of picoline, *tert*-butylpyridine, or quinaldine with tristyrene, as well as in some neat glassformers shown before, and the explanation follows from the correlation between the α-relaxation and the JG β-relaxation or the primitive relaxation of the CM. This feature of the α'-relaxation PVME relaxation is not explainable by the hypothesis of LAC that the α'-relaxation is a confined local relaxation in frozen PS because there is no relation between α'- and α-relaxations in their hypothesis.

From the discussion given above, it is possible that had LAC accepted that the JG β-relaxation is universal but not resolved in neat PVME (just as in picoline, *tert*-butylpyridine, or quinaldine), and it becomes resolved when mixed with another glassformer with much lower mobility, they would have had no need to propose the superfluous concept of confinement in frozen matrix and invent the untenable α'-relaxation. However, their proposal is maintained in a recent study of mixtures of toluene with polychlorinated biphenyl (PCB54) with 0, 20, 35, 50, 70, and 100 wt% of PCB54 by Cangialosi et al. (CAC) [59]. Although the $T_g = 246$ K of pure PCB54 is much higher than the $T_g = 117$ K of toluene, the toluene/PCB54 mixtures are not equivalent in properties to PVME/PS blends or mixtures of tristyrene with picoline, *tert*-butylpyridine, or quinaldine. For one, the higher T_g component PCB54 has much larger dielectric strength than toluene, dominates the loss spectra, and makes it impossible to see the α-relaxation of the toluene component even in mixtures with 20 wt% PCB54. Another difference is that the lower T_g component toluene already has a well-resolved secondary relaxation in isothermal dielectric loss spectra [76, 77], which is the JG β-relaxation because toluene is a rigid molecule, and also its relaxation time is in agreement with the calculated primitive relaxation time of the CM [78]. These undesirable properties should make the toluene/PCB54 mixtures the wrong system to test either the interpretation of LAC or ours. The proposal of LAC would expect a local toluene relaxation, the analogue of the α'-relaxation in PVME/PS blends, with relaxation time having Arrhenius temperature present at temperature below T_{gh} of PCB54 component in the mixture. However, this is hard to verify because toluene already has its JG β-relaxation with the same characteristics. In fact, the local relaxation found in 20, 30, and 50 wt% PCB54 have relaxation times indistinguishable from that of the JG β-relaxation of neat toluene [59]. Our interpretation expects both the α-relaxation and the JG β-relaxation of the toluene component to be present. However, this cannot be checked either because the

α-relaxation of toluene if present would be eclipsed by the dominant PCB54 loss peak in the spectrum.

The ideal system to test the two interpretations involving toluene is mixtures of toluene with polystyrene because the difference between the T_gs of the two components is larger than toluene/PCB54, and PS does not dominate the relaxation spectrum. This system was investigated as early as 1975 by Adachi et al. [79] by dielectric, thermal analysis, and NMR, and they found the primary α-relaxations of toluene and PS together with some local relaxations independent of each other. This study was followed up by others on the same toluene/PS systems by more sophisticated NMR investigations [80]—dielectric and depolarized Rayleigh scattering experiments [81]. In the latter experiment, the two primary α-relaxations of PS and toluene were found over a frequency range of 10 decades, and their relaxation times all have the usual VFTH temperature dependence of cooperative α-relaxations. The same result was found in mixtures of bis(2-ethylhexy1)phthalate with PS [82].

The most recent investigation reported on the toluene/PS mixtures use the sensitive adiabatic calorimetry method in combination with dielectric relaxation. The high molecular mass PS has $T_g = 373$ K, and the difference between T_g of PS and toluene is 256 K. This enormous difference in T_g, together with the absence of domination by the PS contribution in dielectric spectra, are ideal conditions to test both interpretations. In fact, this ideal system has been studied by both adiabatic calorimetry and dielectric measurements by Taniguchi et al. [83]. The measured heat capacity C_p on toluene/PS mixtures containing 20, 30, 40, 50, and 70 wt% PS using an adiabatic calorimeter indicate that the C_p vs temperature T curve exhibit a double-sigmoidal shape. The T_gs corresponding to the two sigmoids are denoted as T_{g1} and T_{g2} with $T_{g1} > T_{g2}$. For the mixture with 70 wt% PS, $T_{g1} = 230$ K is associated with the segmental α-relaxation of the PS component and $T_{g2} = 145$ K is related to the α-relaxation of the toluene component. The difference between the two T_gs decreases with decreasing wt% of PS. For example, the mixture with 30 wt% PS has $T_{g1} = 153$ K and $T_{g2} = 130$ K, and the mixture with 20 wt% PS has $T_{g1} = 135$ K and $T_{g2} = 122$ K. The dielectric measurements found three relaxation processes. The slowest and intermediate processes are identified as the segmental α-relaxation of the PS component, and the rotational α-relaxation of the toluene, respectively. The dielectric T_gs of these two processes, defined as the temperatures at which their dielectric relaxation times attain 10^3 s, agree well with the calorimetric T_{g1} and T_{g2}. From the isochronal loss spectra at 1 kHz of the mixtures, the temperature at the maximum loss of the fastest relaxation is about 110 K and insensitive to composition of the mixture. Converting 1 kHz to time, we find that its relaxation time is 1.6×10^{-4} s at 110 K, which falls on top of the JG β-relaxation times of neat toluene. The reader can easily verify this by inspection of Fig. 4 of CAC. Naturally, the fastest relaxation in the toluene/PS mixtures originates from toluene component. From the calorimetric and dielectric data of the toluene/PS mixtures, Taniguchi et al. found the cooperative rotational α-relaxation of toluene (with VFTH dependence for its relaxation time) and a much faster local relaxation also originating from toluene. For the same reason as given before in the discussion of PVME/PS blends, this similar result again contradict the confinement interpretation of LAC. This is best elucidated by the mixture with 70 wt% PS. Taniguchi et al. [83] still find the cooperative rotational α-relaxation of toluene at $T_{g2} = 145$ K, which is 85 K below the $T_{g1} = 230$ K of the PS component. However, applying the scenario proposed by LAC for PVME/PS to the present case, the PS chains should be frozen at 145 K to confine the toluene, and cooperative motion involving the toluene and PS are not possible except for the local toluene motion confined by the frozen PS chains.

The fact that there are two calorimetric T_gs found by Taniguchi et al. [83] in toluene/PS mixtures is not new. It was found as early as 1965 by Braun and Kovacs [84] also in the same system, and by Plazek et al. in tricresyl phosphate/PS mixtures [85], and in mixtures of PS with dioctyl, dibutyl, or dimethyl phthalate by Savin et al. [86].

Another binary mixture system that supports our interpretation and refutes that of LAC and CAC is the study by Svanberg et al. of propylene carbonate (PC) dissolved in PMMA polymer matrix of a gel consisting of 100% PC down to 50% PC [87]. The difference in T_gs of the two components is about 240 K. The confinement in the gel is of a fractal type with randomly interpenetrating and percolating phases of PMMA and PC. Thus, it is even more appropriate to say that PC is more confined in this system than PVME confined in frozen PS according to LAC, and toluene confined in frozen PCB54 according to CAC. Nevertheless, both the primary α-relaxation and the JG β-relaxation of PC were observed. In neat PC, the JG β-relaxation is not resolved and shows up as an excess wing just as in neat picoline, *tert*-butylpyridine, or quinaldine. On increasing the PMMA content, the α-relaxation of PC is slowed down while the excess wing continuously transforms toward a resolved JG β-relaxation of PC. The effects are similar to that seen in mixtures of picoline, *tert*-butylpyridine, or quinaldine [1–5].

Conclusions

Current research problem of dynamics of water related systems including aqueous mixtures, water under nanoconfinement, and hydrated proteins have been actively pursued using various techniques such as neutron scattering,

dielectric relaxation, and nuclear magnetic resonance. Despite the voluminous amount of data collected by these experimental techniques, no consensus on the interpretation of the observed dynamics has been reached. The recent investigations of these systems by adiabatic calorimetry have significantly clarified the nature of the dynamics, and led to improved understanding of the relaxation processes present. There is also controversy in the interpretation of component dynamics in binary mixtures of two glass-formers. Again, measurements by adiabatic calorimetry have resolved the controversy.

Acknowledgements This study was supported at NRL by the Office of Naval Research, at the Università di Pisa by MIUR-FIRB 2003 D.D.2186 grant RBNE03R78E, and at Tokai University by Grant-in-Aid for Scientific Research (C)(19540429).

References

1. Capaccioli S, Ngai KL, Shinyashiki N. The Johari-Goldstein β-relaxation of water. J Phys Chem B. 2007;111:8197–209.
2. Mierzwa M, Pawlus S, Paluch M, Kaminska E, Ngai KL. Correlation between primary and secondary Johari–Goldstein relaxations in supercooled liquids: invariance to changes in thermodynamic conditions. J Chem Phys. 2008;128:044512.
3. Kessairi K, Capaccioli S, Prevosto D, Lucchesi M, Sharifi S, Rolla PA. Interdependence of primary and Johari-Goldstein secondary relaxations in glass-forming systems. J Phys Chem B. 2008;112:4470–3.
4. Capaccioli S, Prevosto D, Lucchesi M, Rolla PA, Casalini R, Ngai KL. Identifying the genuine Johari-Goldstein β-relaxation by cooling, compressing, and aging small molecular glass-formers. J Non-Cryst Solids. 2005;351:2643–51.
5. Capaccioli S, Kessairi K, Prevosto D, Lucchesi M, Rolla PA. Correlation of structural, Johari-Goldstein relaxations in systems vitrifying along isobaric, isothermal paths. J Phys Condens Matter. 2007;19:205133.
6. Ngai KL. An extended coupling model description of the evolution of dynamics with time in supercooled liquids and ionic conductors. J Phys Condens Matter. 2003;15:S1107–25.
7. Ngai KL, Paluch M. Classification of secondary relaxation in glass-formers based on dynamic properties. J Chem Phys. 2004;120:857.
8. Jansson H, Swenson J. Dynamics of water in molecular sieves by dielectric spectroscopy. Eur Phys J E. 2003;12:S51–4.
9. Bergman R, Swenson J. Dynamics of supercooled water in confined geometry. Nature. 2000;403:283–6.
10. Swenson J, Jansson H, Howells WS, Longeville S. Dynamics of water in a molecular sieve by quasielastic neutron scattering. J Chem Phys. 2005;122:084505.
11. Hedström J, Swenson J, Bergman R, Jansson H, Kittaka S. Does confined water exhibit a fragile-to-strong transition? Eur Phys J. Special Topics. 2007;141:53–6.
12. Faraone A, Liu L, Mou C-Y, Yen C-W, Chen S-H. Fragile-to-strong liquid transition in deeply supercooled confined water. J Chem Phys. 2004;121:10843–6.
13. Liu L, Chen S-H, Faraone A, Yen C-W, Mou C-Y. Pressure dependence of fragile-to-strong transition and a possible second critical point in supercooled confined water. Phys Rev Lett. 2005;95:117802.
14. Mallamace F, Broccio M, Corsaro C, Farone A, Wanderlingh U, Liu L, et al. The fragile-to-strong dynamic crossover transition in confined water: nuclear magnetic resonance results. J Chem Phys. 2006;124:161102.
15. Swenson J. Comment on "Pressure dependence of fragile-to-strong transition and a possible second critical point in supercooled confined water. Phys Rev Lett. 2006;97:189801.
16. Oguni M, Maruyama S, Wakabayashi K, Nagoe A. Glass transitions of ordinary and heavy water within silica-gel nanopores. Chem Asian J. 2007;2:514–20.
17. Debenedetti PG. Supercooled and glassy water. J Phys Condens Matter. 2003;15:R1669–726.
18. Oguni M, Kanke Y, Namba S. Thermal properties of the water confined within nanopores of silica MCM-41. AIP Conf Proc. 2008;982:34.
19. Cammarata M, Levantino M, Cupane A, Longo A, Martorana A, Bruni F. Structure and dynamics of water confined in silica hydrogels: X-ray scattering and dielectric spectroscopy studies. Eur Phys J E. 2003;12:S63–6.
20. Pathmanathan K, Johari GP. Dielectric and conductivity relaxations in Poly(hema) and of water in its hydrogel. J Polym Sci B. 1990;28:675–89.
21. Pathmanathan K, Johari GP. Relaxation and crystallization of water in a hydrogel. J Chem Soc Faraday Trans. 1994;90:1143.
22. Hofer K, Mayer E, Johari GP. Glass liquid transition of water and ethylene-glycol solution in poly(2-hydroxyethyl methacrylate) hydrogel. J Phys Chem. 1990;94:2689–96.
23. Hofer K, Mayer E, Johari GP. Glass liquid transition and calorimetric relaxation of glassy aqueous-solutions imbibed in poly(2-hydroxyethyl methacrylate)—a comparison with bulk behavior. J Phys Chem. 1991;95:7100.
24. Johari GP, Hallbrucker A, Mayer E. The glass liquid transition of hyperquenched water. Nature. 1987;330:552–3.
25. Johari GP, Hallbrucker A, Mayer E. Isotope effect on the glass-transition and crystallization of hyperquenched glassy water. J Chem Phys. 1990;92:6742–6.
26. Johari GP, Astl G, Mayer E. Enthalpy relaxation of glassy water. J Chem Phys. 1990;92:809–10.
27. Swenson J, Jansson H, Hedström J, Bergman R. Properties of hydration water, its role in protein dynamics. J Phys Condens Matter. 2007;19:205109.
28. Shinyashiki N, Yamamoto W, Yokoyama A, Yoshinari T, Yagihara S, Kita R, Ngai KL, Capaccioli S. Glass transitions in aqueous solution of protein (bovine serum albumin). J Phys Chem B. 2009;113:14448.
29. Kawai K, Suzuki T, Oguni M. Low-temperature glass transitions of quenched and annealed bovine serum albumin aqueous solutions. Biophys J. 2006;90:3732–8.
30. Doster W, Settles M. Protein-water displacement distributions. Biochim Biophys Acta. 2005;1749:173–86.
31. Doster W. The dynamical transition of proteins, concepts and misconceptions. Eur Biophys J. 2008;37:591–602.
32. Parak F, Knapp EW, Kucheida D. Protein dynamics Mössbauer spectroscopy on deoxymyoglobin crystals. J Mol Biol. 1982;161:177–94.
33. Doster W, Cusak S, Petry W. Dynamical transition of myoglobin revealed by inelastic neutron scattering. Nature. 1989;337:754–6.
34. Chen S-H, Liu L, Fratini E, Baglioni P, Faraone A, Mamontov E. Observation of fragile-to-strong dynamic crossover in protein hydration water. Proc Natl Acad Sci USA. 2006;103:9012–6.
35. Khodadadi S, Pawlus S, Roh JH, Garcia Sakai V, Mamontov E, Sokolov AP. The origin of the dynamic transition in proteins. J Chem Phys. 2008;128:195106.
36. Khodadadi S, Pawlus S, Sokolov AP. Influence of hydration on protein dynamics: combining dielectric and neutron scattering spectroscopy data. J Phys Chem B. 2008;112:14273–80.

37. Tarek M, Tobias DJ. Role of protein-water hydrogen bond dynamics in the protein dynamical transition. Phys Rev Lett 2002;88:138101.
38. Ringe D, Petsko GA. The 'glass transition' in protein dynamics: what it is, why it occurs, and how to exploit it. Biophys Chem. 2003;105:667–80.
39. Miyazaki Y, Matsuo T, Suga H. Low-temperature heat capacity and glassy behavior of lysozyme crystal. J Phys Chem B. 2000;104:8044–52.
40. Teeter MM, Yamano A, Stec B, Mohanty U. On the nature of a glassy state of matter in a hydrated protein: relation to protein function. Proc Natl Acad Sci USA. 2001;98:11242–7.
41. Zanotti J-M, Gibrat G, Bellissent-Funel M-C. Hydration water rotational motion as a source of configurational entropy driving protein dynamics. Crossovers at 150 and 220 K. Phys Chem Chem Phys. 2008;10:4865.
42. Fenimore PW, Frauenfelder H, McMahon BH, Young RD. Bulk-solvent and hydration-shell fluctuations, similar to α- and β-fluctuations in glasses, control protein motions and functions. Proc Natl Acad Sci USA. 2004;101:14408–13.
43. Ngai KL. Dynamic and thermodynamic properties of glass-forming substances. J Non-Cryst Solids. 2000;275:7–51.
44. Casalini R, Ngai KL. Structural dependence of fast relaxation in glass-forming substances and correlation with the stretch exponent of the slow structural α-relaxation. J Non-Cryst Solids. 2001;293–295:318–26.
45. Angell CA. Ten questions on glassformers, and a real space 'excitations' model with some answers on fragility and phase transitions. J Phys Condens Matter. 2000;12:6463–75.
46. Sokolov AP, Kisliuk A, Novikov VN, Ngai KL. Observation of constant loss in fast relaxation spectra of polymers. Phys Rev B. 2001;63:172204.
47. Kisliuk A, Novikov VN, Sokolov AP. Constant loss in Brillouin spectra of polymers. J Polym Sci B. 2002;40:201–9.
48. Ngai KL. Why the fast relaxation in the picosecond to nanosecond time range can sense the glass transition. Philos Mag. 2004;84:1341–53.
49. Capaccioli S, Shahin Thayyil M, Ngai KL. Critical issues of current research on the dynamics leading to glass transition. J Phys Chem B. 2008;112:16035–49.
50. Ngai KL, Habasaki J, Leon C, Rivera A. Comparison of dynamics of ions in ionically conducting materials and dynamics of glass-forming substances: remarkable similarities. Z Phys Chem. 2005;219:47.
51. Nowaczyk A, Geil B, Hinze G, Böhmer R. Correlation of primary relaxations and high-frequency modes in supercooled liquids. II. Evidence from spin-lattice relaxation weighted stimulated-echo spectroscopy. Phys Rev E. 2006;74:041505.
52. Lusceac S, Vogel MR, Herbers CR. ^{2}H and ^{13}C NMR studies on the temperature-dependent water and protein dynamics in hydrated elastin, myoglobin and collagen. arXiv:0904.4424v1 [cond-mat.soft]. Accessed 28 April 2009.
53. Döß A, Paluch M, Sillescu H, Hinze G. From strong to fragile glass formers: secondary relaxation in polyalcohols. Phys Rev Lett. 2002;88:095701.
54. Morozov VN, Gevorkian SG. Low-temperature glass transition in proteins. Biopolymers. 1985;24:785.
55. Ngai KL, Capaccioli S, Shinyashiki The N. Protein "glass" transition, the role of the solvent. J Phys Chem B. 2008;112:3826.
56. Ngai KL, Capaccioli S, Shinyashiki N, Shahin Thayyil M. Recent progress in understanding relaxation in complex systems. J Non-Cryst Solids. in press.
57. Gainaru C, Fillmer A, Böhmer R. Surface activation by deeply supercooled hydration water in connective tissue proteins. J Phys Chem B 2009; Submitted.
58. Lorthioir C, Alegrıa A, Colmenero J. Out of equilibrium dynamics of poly(vinyl methyl ether) segments in miscible poly(styrene)-poly(vinyl methyl ether) blends. Phys Rev E. 2003;68:031805.
59. Cangiolosi D, Alegria A, Colmenero J. Dielectric relaxation of polychlorinated biphenyl/toluene mixtures: component dynamics. J Chem Phys. 2008;128:224508.
60. Urakawa O, Fuse Y, Hori H, Tran-Cong Q, Yano O. A dielectric study on the local dynamics of miscible polymer blends: poly (2-chlorostyrene)/poly(vinyl methyl ether). Polymer. 2001;42: 765–73.
61. Miwa Y, Usami K, Yamamoto K, Sakaguchi M, Sakai M, Shimada S. Direct detection of effective glass transitions in miscible polymer blends by temperature-modulated differential scanning calorimetry. Macromolecules. 2005;38:2355–61.
62. Kahle S, Korus J, Hempel E, Unger R, Höring S, Schröter G, et al. Glass-transition cooperativity onset in a series of random copolymers poly(n-butyl methacrylate-stat-styrene). Macromolecules. 1997;30:7214–23.
63. Ngai KL. Correlation between β-relaxation and α-relaxation in the family of poly(n-butyl methacrylate-stat-styrene) random copolymers. Macromolecules. 1999;32:7140–6.
64. Miller JB, McGrath KJ, Roland CM, Trask CA, Garroway AN. Nuclear magnetic resonance study of polyisoprene/poly(vinylethylene) miscible blends. Macromolecules. 1990;23:4543–7.
65. Alegria A, Colmenero J, Ngai KL, Roland CM. Observation of the component dynamics in a miscible polymer blend by dielectric, mechanical spectroscopies. Macromolecules. 1994;27: 4486.
66. Ngai KL, Roland CM. Component dynamics in polyisoprene/poly(vinylethylene) blends. Macromolecules. 1995;28:4033–5.
67. Chung G-C, Kornfield JA, Smith SD. Compositional dependence of segmental dynamics in a miscible polymer blend. Macromolecules. 1994;27:5729–41.
68. Sakaguchi T, Taniguchi N, Urakawa O, Adachi K. Calorimetric study of dynamical heterogeneity in blends of polyisoprene and poly(vinylethylene). Macromolecules. 2005;38:422–8.
69. Lodge TP, Wood ER, Haley JC. Two calorimetric glass transitions do not necessarily indicate immiscibility: the case of PEO/PMMA. J Polym Sci B. 2006;44:756–63.
70. Ngai KL, Roland CM. Models for the component dynamics in blends and mixtures. Rubber Chem Technol. 2004;77:579–90.
71. Roland CM, McGrath KJ, Casalini R. Dynamic heterogeneity in poly(vinyl methyl ether)/poly(2-chlorostyrene) blends. Macromolecules. 2006;39:3581–7.
72. Lutz TR, He Y, Ediger MD, Cao H, Lin G, Jones AA. Rapid poly(ethylene oxide) segmental dynamics in blends with poly (methyl methacrylate). Macromolecules. 2003;36:1724–30.
73. Ngai KL, Roland CM. Unusual component dynamics in poly(ethylene oxide)/poly(methyl methacrylate) blends as probed by deuterium NMR. Macromolecules. 2004;37:2817–22.
74. Ngai KL. Predicting the changes of relaxation dynamics with various modifications of the chemical and physical structures of glass-formers. J Non-Cryst Solids. 2007;353:4237–45.
75. Jin X, Zhang S, Runt J. Broadband dielectric investigation of amorphous poly(methyl methacrylate)/poly(ethylene oxide) Blends. Macromolecules. 2004;37:8110–5.
76. Doss A, Hinze G, Schiener B, Hemberger J, Böhmer R. Dielectric relaxation in the fragile viscous liquid state of toluene. J Chem Phys. 1997;107:1740.
77. Kudlik A, Benkhof S, Blochowicz T, Tschirwitz C, Rossler E. The dielectric response of simple organic glass formers. J Mol Liq. 1999;479:201.
78. Hensel-Bielowka S, Paluch M, Ngai KL. Emergence of the genuine Johari–Goldstein secondary relaxation in m-fluoroaniline

after suppression of hydrogen-bond-induced clusters by elevating temperature and pressure. J Chem Phys. 2005;123:014502.
79. Adachi K, Fujihara I, Ishida Y. Diluent effects on molecular motions and glass transition in polymers. I. Polystyrene-toluene. J Polym Sci Polym Phys Ed. 1975;13:2155–71.
80. Rössler E, Sillescu H, Spiess HW. Deuteron NMR in relation to the glass transition in polymers. Polymer. 1985;26:203–7.
81. Floudas G, Steffen W, Fischer EW, Brown W. Solvents and polymer dynamics in concentrated polystyrene/toluene solutions. J Chem Phys. 1993;99:695.
82. Rizos AK, Johnsen RM, Brown W, Ngai KL. Component dynamics in polystyrene/bis(2-ethylhexyl) phthalate solutions by polarized and depolarized light scattering and dielectric spectroscopy. Macromolecules. 1996;28:5450–7.
83. Taniguchi N, Urakawa O, Adachi K. Calorimetric study of dynamical heterogeneity in toluene solutions of polystyrene. Macromolecules. 2004;37:7832–8.
84. Braun G, Kovacs AJ. Variations de la temperature de transition vitreuse du polystyrolene en fonction de la concentration en plastifiant. Compte Rendus. 1965;260:2217–20.
85. Plazek DJ, Riande E, Markovitz H, Raghupathi N. Concentration dependence of the viscoelastic properties of polystyrene-tricresyl phosphate solutions. J Polym Sci Polym Phys Ed. 1979;17:2189.
86. Savin DA, Larson AM, Lodge TP. Effect of composition on the width of the calorimetric glass transition in polymer-solvent and solvent-solvent mixtures. J Polym Sci B. 2004;42:1155–63.
87. Svanberg C, Bergman R, Jacobsson P. Secondary relaxation in confined and bulk propylene carbonate. Europhys Lett. 2003;64:358–63.